ORIGINAL PAPER

Photofunctional Polyurethane Nanofabrics Doped by Zinc Tetraphenylporphyrin and Zinc Phthalocyanine Photosensitizers

Jiří Mosinger · Kamil Lang · Pavel Kubát · Jan Sýkora · Martin Hof · Lukáš Plíštil · Bedřich Mosinger Jr.

Abstract Polymeric polyurethane nanofabrics doped by zinc tetraphenylporphyrin (ZnTPP) and/or zinc phthalocyanine (ZnPc) photosensitizers were prepared by the electrospinning method and characterized by microscopic methods, steady-state and time-resolved fluorescence, and absorption spectroscopy. Nanofabrics doped by both ZnTPP and ZnPc efficiently harvest visible light to generate triplet states and singlet oxygen $O_2(^1\Delta_g)$ with a lifetime of about 15 μs in air atmosphere. The energy transfer between the excited singlet states of ZnTPP and ground states of ZnPc is described in details. All nanofabrics have bactericidal surfaces and photooxidize inorganic and organic substrates. ZnTPP and ZnPc in the polyurethane nanofabrics are less photostable than incorporated free-base tetraphenylporphyrin (TPP).

Introduction

New antibacterial strategies are required in view of the increasing resistance of bacteria to antibiotics. Photodynamic killing of bacteria utilizes light in the combination with a photosensitizer (drug) to induce phototoxic reactions [1] identical to the use of photodynamic therapy of cancer [2]. The general mechanism of phototoxic reaction starts by absorption of photon(s) by a photosensitizer followed by intersystem crossing from the excited singlet state to the low-lying triplet state [3, 4]. A triplet photosensitizer can attack target species directly (redox or free radical reaction, type I mechanism) or transfer its energy to an oxygen molecule. The lowest excited state of singlet oxygen, $O_2(^1\Delta_g)$, formed is very reactive and can oxidize target species especially containing C=C bonds (type II mechanism) [5–7].

Recently, new polymeric materials with photodynamic activity were applied for fabrication of the intraocular lenses having the bactericidal surface [8, 9]. In our previous study we have prepared polymeric nanofabrics doped by the 5,10,15,20-tetraphenylporphyrin photosensitizer (TPP, Fig. 1) [10]. Such self-disinfecting nanofabrics are promising materials for the preparation of wound dressing or filters for water treatment. TPP and other porphyrins have a strong blue absorption band, however, the absorption in other parts of the visible spectra is limited. To overcome

J. Mosinger (✉)
Faculty of Science, Charles University in Prague,
Hlavova 2030,
128 40 Praha 2, Czech Republic
e-mail: mosinger@natur.cuni.cz

J. Mosinger · K. Lang
Institute of Inorganic Chemistry, v.v.i.,
Academy of Sciences of the Czech Republic,
250 68 Řež, Czech Republic

P. Kubát (✉) · J. Sýkora · M. Hof
J. Heyrovský Institute of Physical Chemistry, v.v.i.,
Academy of Sciences of the Czech Republic,
Dolejškova 3,
18223 Praha 8, Czech Republic
e-mail: pavel.kubat@jh-inst.cas.cz

L. Plíštil
Elmarco, s.r.o.,
V Horkách 76/18,
460 07 Liberec 9, Czech Republic

B. Mosinger Jr.
Mount Sinai School of Medicine,
1425 Madison Avenue,
New York, NY 10029, USA

Fig. 1 Structure of TPP, ZnTPP, and ZnPc
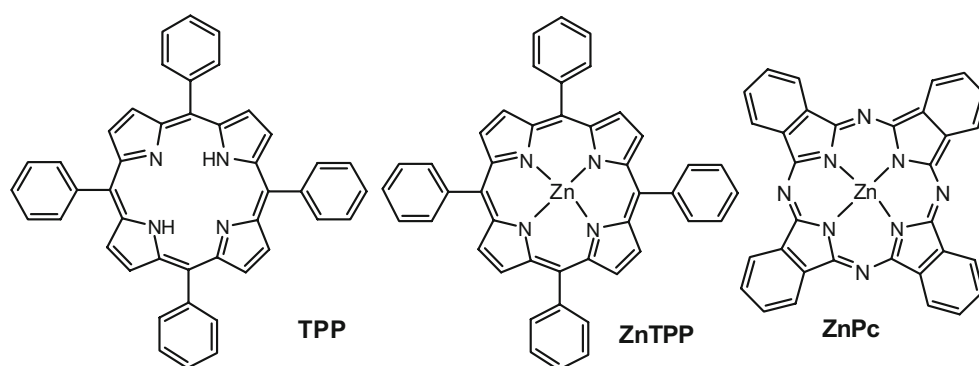
these difficulties in light harvesting we have prepared and characterized a set of nanofabrics doped by two photo-sensitizers: zinc(II) 5,10,15,20-tetraphenylporphyrin (ZnTPP) and/or zinc(II) phthalocyanine (ZnPc) (Fig. 1). Porphyrin ZnTPP has the strongest absorption in the Soret band around 420 nm, whereas ZnPc absorbs strongly up to 670 nm (Q-band). Thus, a broad range of the solar spectrum or white light is absorbed by mixed ZnTPP and ZnPc compounds.

In nonpolar solvents, both ZnTPP and ZnPc are efficiently excited to the triplet states and produce O_2 ($^1\Delta_g$) with the quantum yields of the singlet oxygen formation, Φ_Δ, above 0.5 [11]. The presence of central zinc atom prevents protonation of the pyrrole nitrogens, the process that affects Φ_Δ [12]. The photophysical data are valid for monomeric species. The aggregation of porphyrins and phthalocyanines is not desirable since their phototoxicity decreases as a result of the poor or absent ability of dimers and higher aggregates to produce O_2 ($^1\Delta_g$) [4, 13]. The inherent photophysical and photochemical properties can be altered because the photosensitizers are constrained within the environment of a polymeric matrix and, therefore, the photoactivity of the resulting material cannot be directly extrapolated from the known behavior in a solution [4].

In this paper we present the preparation of novel polyurethane (PUR) nanofabrics doped by ZnTPP and ZnPc and the properties based on steady-state and time-resolved fluorescence and absorption measurements. We demonstrate the ability of the nanofabrics to photooxidize organic and inorganic compounds and their antibacterial activity. The results are compared with those of nanofabrics doped by TPP [10].

Materials and methods

Chemicals

Zinc(II) 5,10,15,20-tetraphenylporphyrin (ZnTPP) (Porphyrin Systems, Germany), zinc(II) phtalocyanine (ZnPc), 5,10,15,20-tetraphenylporphyrin (TPP) (Sigma-Aldrich), 2-dodecyloxyethanol (Slovasol S), toluene (all Penta,

Czech Republic), 5-bromo-4-chloro-3-indolyl-β-D-galacto-pyranoside (X-gal, Invitrogen, CA, USA); *Escherichia col* *i*DH5α (Invitrogen, CA, USA); Plasmid pGEM11Z (Promega, WI, USA); sodium salt of uric acid, N,N-dimethylfor-mamide (DMF), KI, and other inorganic salts (all Aldrich) were used as received. Polyurethane Larithane LS 1086 (Mw≈50000, 30% solution in DMF) purchased from Novotex (COIM SpA) is an aliphatic elastomer based on linear polycarbonated diol, isophorone diisocyanate, and extended isophorone diamine. The composition of polymer solutions used for the polyurethane nanofiber (PUR) preparation is as follows: 15% Larithane in DMF, 0.6% Slovasol S, 0.1% TPP, ZnTPP, or ZnPc in DMF by the polymer weight.

Preparation of nanofabrics

Nanofibrous layers were produced using the Nanospider™ electrospinning technology (Fig. 2a) [14]. A cylindrical-shape spinning electrode connected with a high voltage source rotated in a polymer solution. A highly charged thin layer of the solution on the electrode surface was then transformed into nanofibers, which were collected on a linearly moving grounded polypropylene spunbond textile. The distance between the electrodes varied from 15 to 19 cm and the input voltage varied from 70 kV to 80 kV. The area weight of obtained nanofibrous layers was kept at 2 g/m² with a thickness of 0.03 mm and the fiber diameter varying between 200 and 500 nm (Fig. 2b).

Steady-state absorption and fluorescence spectroscopy

The UV/VIS absorption spectra were recorded using a Perkin Elmer Lambda 19, Perkin Elmer Lambda 35, and Unicam 340 spectrometers. The fluorescence spectra were measured on a Perkin–Elmer LS 50B luminescence spectrophotometer. All fluorescence emission spectra were corrected for the characteristics of the detection monochro-mator and photomultiplier using the fluorescence standards. The samples were excited at the band maxima of ZnPc (671 nm) and ZnTPP (427 nm).

Fig. 2 Nanospider™ electro-spinning technology (**a**) and scanning electron microscopy image of the resulting nanofibers doped by ZnTPP (**b**)
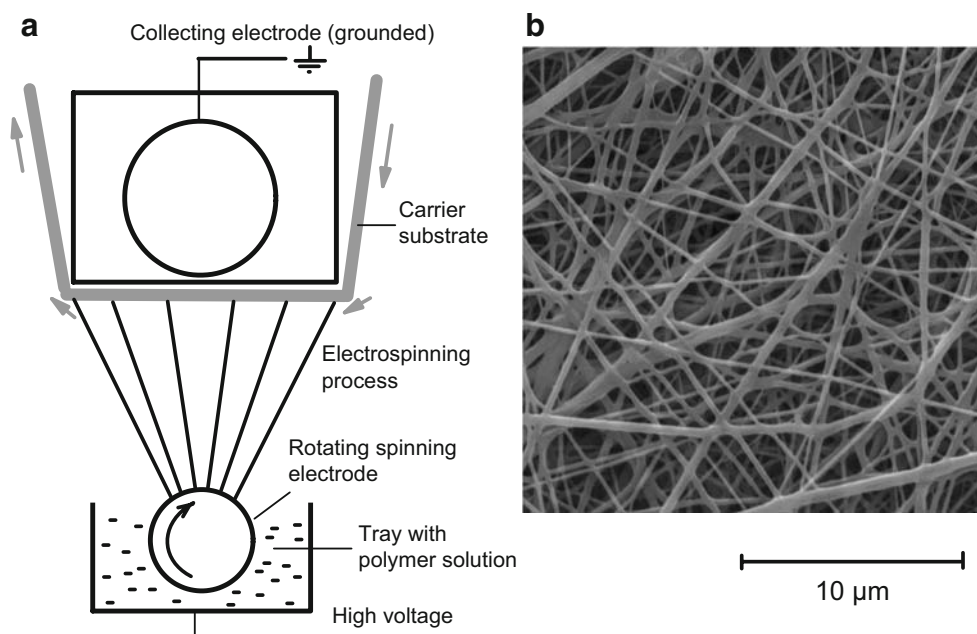
Time correlated single photon counting (TCSPC)

The fluorescence lifetimes were measured on a 5,000 U Single Photon Counting instrument (IBH, U.K.) using PicoQuant laser diodes LDH-P-C-405 (405 nm peak wavelength, pulse width <100 ps, 2.5 MHz repetition rate) and LDH-P-635 (635 nm peak wavelength, pulse width <150 ps, 2.5 MHz repetition rate) (PicoQuant, Germany), and a cooled Hamamatsu R3809U-50 microchannel plate photomultiplier. Decay curves were recorded at the maxima of the steady-state fluorescence spectra of the individual systems. The fluorescence wavelengths were selected by a monochromator. Additionally, two filters were used to eliminate scattered light of a blue (a 550 nm cut off filter) and a red (a 650 nm cut off filter) laser diode. The data were collected in 4,096 channels (0.028 ns per channel) till the peak value reached 5,000 counts. The decay curves were fitted to multiexponential functions performing the iterative reconvolution procedure of the IBH DAS6 software. The resolution time is about 50 ps.

Confocal fluorescence and fluorescence lifetime imaging microscopy (FLIM)

The measurements were carried out on an inverted epifluor-escence confocal microscope MicroTime 200 (PicoQuant, Germany). We used configuration containing a pulsed diode laser (LDH-P-C-405, 405 nm, PicoQuant) providing 80 ps pulses at 40 MHz repetition rate, dichroic mirror 505DRLP, long-pass filter LP500 (Omega Optical), water immersion objective (1.2 NA, 60x) (Olympus), and detector PDM SPAD (MPD, USA). A module Picoharp 300 (PicoQuant, Germany) recorded the photon events in a TTTR mode enabling

the reconstruction of the lifetime histogram for each pixel [15]. In order to minimize the pile-up effects low power of 1.5 μW at the back aperture of the objective was chosen.

Transient absorption measurements

Laser flash photolysis experiments were performed using a Lambda Physik COMPEX102 excimer (308 nm) and an FL 3002 dye laser (425 nm for excitation of ZnTPP, 658 nm for excitation of ZnPc, output 0.05–3 mJ/pulse, pulse width 28 ns). Transient absorption spectra (300–800 nm) were recorded using a laser kinetic spectrometer LKS 20 (Applied Photophysics, UK). The time profiles of the triplet state decay were recorded at 460–500 nm using a 250 W Xe lamp equipped with a pulse unit and a R928 photomultiplier (Hamamatsu). The lifetimes of the ZnPc and ZnTPP triplet states (τ_T) were obtained by a single exponential fitting to the decay curves measured in argon-saturated solutions and averaged from at least five measurements. The quenching rate constants of the triplet states by oxygen (k_q) were calculated using a least-square linear fit to the rate constants of the triplet states deactivation in argon, air, and oxygen atmosphere.

Phosphorescence of $O_2(^1\Delta_g)$

Time-resolved near-infrared phosphorescence of O_2 $(^1\Delta_g)$ at 1,270 nm was observed at the right angle to an excitation pulse (the same lasers as for transient absorption measurements) using a homemade detector unit (interference filter, Ge diode Judson J16-8SP-R05M-HS). The samples were placed in a 10 mm quartz cell saturated with oxygen, air, or argon. Used incident energy is within the energy region

where the intensity of a phosphorescence signal is directly proportional to the incident energy (less than 1 mJ).

Continuous irradiation

A piece of the nanofabric was peeled off from a polypropylene supporting textile, coiled around a quartz plate ($10 \times 40 \times 1$ mm), and put into a thermostated 10 mm quartz cell (22 °C) containing a substrate aqueous solution (0.1 M I^- or 10^{-4} M sodium salt of uric acid). The cell was irradiated by a 300 W stabilized halogen lamp with or without an attenuator under continuous stirring. The UV/VIS absorbance changes due to the formation of oxidized products were recorded in regular time intervals and compared with those of a blank solution of the same composition kept in the dark.

Biological experiments

A piece of the photosensitizer-doped nanofabric was placed on X-gal (80 μg/ml) bacterial agar LB plates and inoculated with one or two drops of bacteria *Escherichia coli* DH5α containing plasmid pGEM11Z producing β-galactosidase. The bacterial concentration was typically chosen such that 10 μl contained approximately several hundred bacteria able to form colonies. 5 to 25 μl of the bacterial suspension was pipetted on the nanofabrics. The agar plates were either illuminated with cold white light of a 150 W halogen bulb for 30 min, or kept in the dark. The plates were then incubated overnight in the dark at 37 °C to allow individual bacteria to grow into visible blue-green colonies. Blue-green color of the colonies is due to an indol dye produced from X-gal substrate (5-bromo-4-chloro-3-indolyl-β-D gal-actopyranoside) by bacterial β-galactosidase.

Results and discussion

We have studied four PUR nanofabrics containing 0.1% ZnPc (**1**), 0.1% ZnTPP (**2**), and the mixture of 0.1% ZnPc and 0.1% ZnTPP (**3**), while **4** consists of two independent layers of nanofibres, one layer is doped by 0.1% ZnPc and second layer by 0.1% ZnTPP. A control PUR nanofabric without photosensitizers was used in biological experiments.

UV/Vis absorption spectra

The UV/VIS spectrum of nanofabric **1** shows the characteristic Q absorption bands of ZnPc at 672, 641, and 605 nm (Fig. 3a). Nanofabric **2** with ZnTPP has the Soret band at 427 nm and the two Q bands at 560 and 601 nm (Fig. 3b). The bands are red shifted by several nm when compared with those recorded in nonpolar solvents. It has
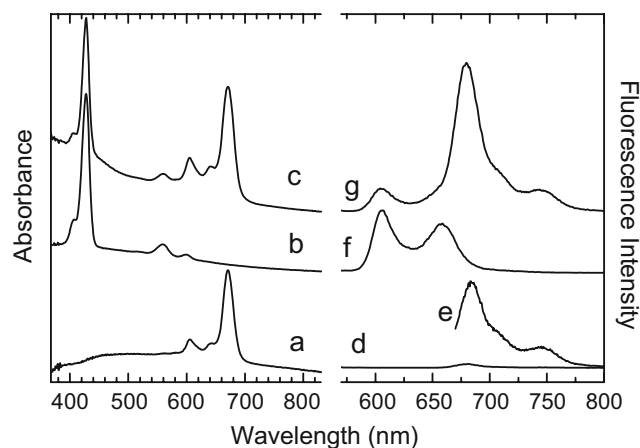
Fig. 3 Absorption spectra of nanofabric **1** (**a**), **2** (**b**), and **3** (**c**). Corrected fluorescence emission spectra of **1** (**d**), **2** (**f**), and **3** (**g**) excited at the Soret band maximum of ZnTPP (427 nm) and **1** (**e**) excited at the band of ZnPc (671 nm). Spectra are offset

been recognized that solvent-dependent red shifts in the absorption spectra of zinc porphyrins arise from the axial ligation by solvent molecules to form five-coordinate zinc complexes [16, 17]. Similar red shifts were observed for zinc porphyrin attached covalently to polyamide dendrimer whereas no shifts were found for free-base porphyrin [18]. Thus, the red shifts of approximately 7 nm in the Soret and Q-band regions of ZnTPP in **2** can be attributed to an interaction of lone pair electrons of the polymer imide or carbonyl groups with porphyrin zinc atoms. The explanation is supported by the fact that the TPP absorption bands do not shift upon the encapsulation in PUR nanofabrics [10]. The effects of the ligation can be also responsible for a small shift of ZnPc absorption bands in different solvents [19] and in the PUR matrix of **1**.

The absorption spectra of nanofabrics **3** (Fig. 3c) and **4** are the pure superpositions of the respective spectra of **1** and **2** suggesting negligible interaction between the porphyrin and phthalocyanine moieties in the ground state. Similarly to the spectra of porphyrin - phthalocyanine composites [20] there are no shifts and broadening of the bands when compared to the spectra of **1** and **2**.

Aggregation of porphyrins and phthalocyanines is characterized by a splitting and/or broadening of the bands in UV/Vis spectra [21]. Our observations (Fig. 3a–c) indicate that ZnPc and ZnTPP incorporated in PUR nanofibers **1**–**4** remain in the monomeric state and interact with polymer *via* the ligation of zinc atoms with the imide or carbonyl groups of the PUR matrix.

Steady-state and time-resolved fluorescence spectra

Similarly to the absorption spectra, the steady-state fluorescence emission bands are red shifted by 8–10 nm when compared with the measurements in nonpolar solvents. The

bands maxima are at 685, 746 nm and 606, 658 nm for ZnPc in nanofabric **1** (Fig. 3e) and ZnTPP in nanofabric **2** (Fig. 3f), respectively. Since the absorption Q-band of ZnPc (672 nm) overlaps the fluorescence emission band of ZnTPP, fluorescence resonance energy transfer from the porphyrin excited singlet states to phthalocyanine can occur in nanofabrics **3** (Fig. 3g) and **4**.

The time evolution of fluorescence was investigated by TCSPC. As shown above ZnTPP is the dominant absorber at 427 nm with dominant fluorescence at 606 and 658 nm whereas ZnPc is the dominant absorber at 672 nm with dominant fluorescence above 680 nm (Fig. 3). Therefore, the decay curves obtained after 405 nm excitation were recorded at the emission wavelengths set to 600 (ZnTPP fluorescence) or 700 nm (ZnPc fluorescence). All fluorescence decay curves were fitted to a one- or two-exponential decay model using a nonlinear least-squares curve-fitting algorithm.

The fluorescence emission of ZnTPP in nanofabric **2** is characterized by a fast increase followed by two exponen-
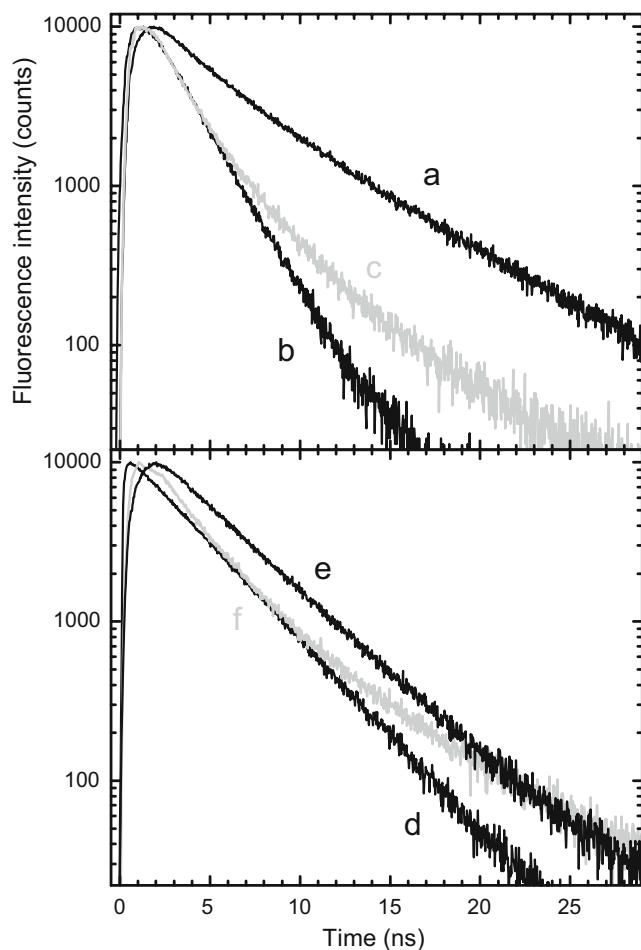
Fig. 4 Time-resolved fluorescence of ZnTPP measured at 600 nm in nanofabric **2** (**a**), **3** (**b**), and **4** (**c**, *grey line*). Time-resolved fluorescence of ZnPc at 700 nm in nanofabric **1** (**d**), **3** (**e**), and **4** (**f**, *grey line*). Excitation wavelength was set to 635 nm for nanofabrics **1** and 405 nm for nanofabrics **2**, **3**, and **4**

tial decay process with lifetimes of 2.9 (40%) and 6.9 ns (60%) (Fig. 4a). Strong quenching of ZnTPP fluorescence by ZnPc was observed in nanofabrics **3** and **4** (Fig. 4b, c). To quantify differences in fluorescence quenching, the average fluorescence lifetimes were calculated as $\tau_F = \sum_i A_i \tau_i^2 \big/ \sum_i A_i \tau_i$, where τ_i are the lifetimes and A_i the corresponding amplitudes [22].

Fluorescence resonance energy transfer occurs when the electronic excitation energy of a donor chromophore is transferred to an acceptor molecule nearby *via* a dipole–dipole interaction within a donor–acceptor pair. Fig. 3 shows a sufficient overlap between the emission band of ZnTPP and the absorption band of ZnPc. As a result, effective energy transfer between ZnTPP and ZnPc occurs with an estimated efficiency of about 70% in nanofabric **3**. Since the efficiency is higher than 50% the distance between both chromophores is closer than 5 nm on average, the value of the Förster distance calculated for a zinc porphyrin-phthalocyanine pair [20]. The efficiency of the energy transfer becomes significantly lower in nanofabric **4** (*cf.* Fig. 4b, c) with the decay curves indicating two populations of donor ZnTPP molecules (Fig. 4c). The long-lived component can be attributed to the molecules, which do not undergo energy transfer, and thus are separated by a significantly higher distance than the Förster radius. The other fraction of the ZnTPP molecules shows a shortening of the lifetime due to FRET. These molecules are located probably in the nodes, where the nanofibers labeled with ZnPc and ZnTPP are in the close contact.

Fluorescence emission of ZnPc in nanofabric **1** decays monoexponentially with a lifetime of 3.6 ns (Fig. 4d). The slower kinetics of the ZnPc fluorescence decay in **3** and **4** reflect energy transfer from ZnTPP excited singlet states (Fig. 4e, f).

Confocal fluorescence and fluorescence lifetime imaging microscopy

The recorded intensity image of ZnTPP emission in nanofabric **2** is shown in Fig. 5a depicting the labeling of the individual fibers. The incorporation of ZnTPP and ZnPc in the PUR nanofibres was also investigated by FLIM. To characterize fluorescence decays recorded for each pixel, the average lifetimes are calculated as $\tau_{av} = \sum I_i t_i / \sum I_i$, where I_i and t_i are the intensity and time corresponding to the *i*-th channel in the time-correlated single photon counting histogram, respectively. The average lifetime distribution fulfills the Gaussian model, yielding a mean lifetime as shown in the right panel of Fig. 5. Nanofabric **3** (Fig. 5d) doped with the mixture of ZnTPP and ZnPc has the average lifetime significantly reduced compared to nanofabric **2** (Fig. 5c), nevertheless its value is higher than

Fig. 5 Fluorescence intensity image of nanofabric **2** (**a**). Distribution of the average fluorescence lifetimes, τ_{av}, of ZnPc in **1** (**b**), ZnTPP in **2** (**c**), and ZnPc and ZnPc in **3** (**d**). The emission wavelengths were above 550 nm as selected by a cut-off filter; the arrow indicates the direction of energy transfer
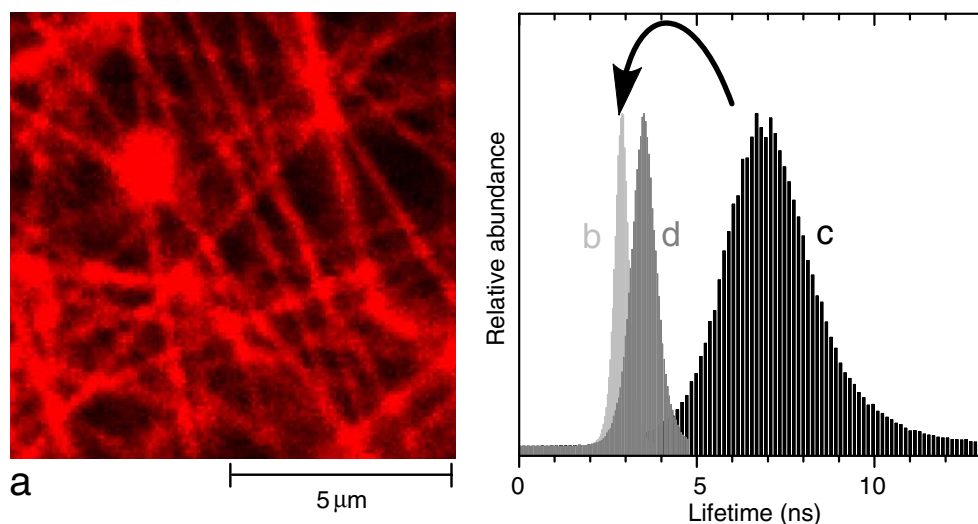
that of nanofabric **1** containing only ZnPc (Fig. 5b). These results correlate with the lifetimes evaluated from TCSPC measurements (see above) and also prove energy transfer occurring between the excited ZnTPP singlet states and the ZnPc chromophore.

Triplet–triplet absorption spectra

The transient absorption spectra of ZnPc in **1** (Fig. 6a) and ZnTPP in **2** (Fig. 6b) show typical broad absorption maxima at 460–500 nm not affected by the interaction with the PUR matrix. These spectral features are indicative of the ZnTPP and ZnPc triplet states [23]. In air atmosphere the triplet states of ZnTPP and ZnPc are quenched by oxygen monoexponentially with a lifetime of 29±5 μs. The increase of the triplet lifetimes when compared to a solution (~ 2 μs) can be attributed to a combination of several factors including changes in the ZnTPP and ZnPc microenvironment due to the sensitizer accommodation within the non-polar matrix and in the reduced exposure of the triplet states to oxygen [4]. The lifetime of the triplet states, τ_T, in argon atmosphere, and the quenching rate constants of the triplet states by oxygen, k_q, are summarized in Table 1. The comparable values of k_q indicate the similar diffusivity of oxygen in all prepared PUR nanofabrics.
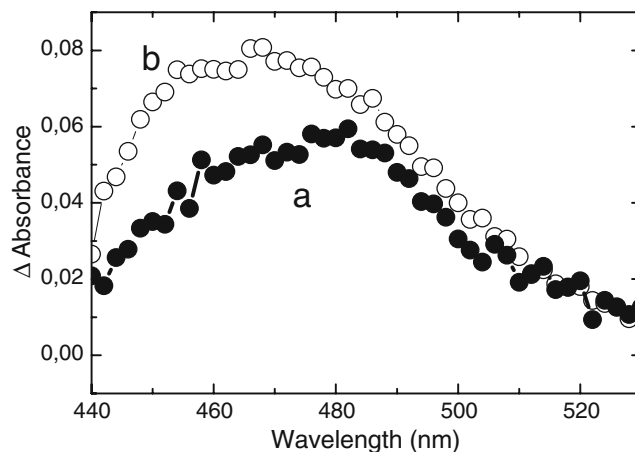
The triplet states of ZnPc and ZnTPP in nanofabrics **3** and **4** cannot be differentiated due to the similar transient absorption spectra (Fig. 6a, b) and the photophysical behavior (Table 1). We suppose that the ZnPc singlet states, the predecessor of the triplet states, are created partly by direct excitation of ZnPc and partly by energy transfer from the ZnTPP excited singlet states. Also the formation of the ZnPc triplet states ($E_{triplet}=1.12$ eV) by energy transfer from the ZnTPP triplets ($E_{triplet}=1.53$ eV) cannot be excluded [24].

Singlet oxygen $O_2(^1\Delta_g)$

The recorded phosphorescence at 1,270 nm belongs to $O_2(^1\Delta_g)$ on the basis of the observed wavelength, the signal disappearance after purging the sample with argon, and the signal reappearance after the addition of air or oxygen. The fast signal at the beginning of the curve (0–1 μs) remains even in argon atmosphere and belongs to sensitizer fluorescence and light scattering of the excitation laser pulse. The formation of $O_2(^1\Delta_g)$ reflects the kinetics of the triplet states quenching by ground state $O_2(^3\sum_g)$. Kinetic traces were fitted using Eq. (1) where the lifetime of $O_2(^1\Delta_g)$, τ_Δ, and the amplitude A are free parameters

$$S(t) = A \frac{\tau_\Delta}{\tau_T - \tau_\Delta}(\exp(-t/\tau_T) - \exp(-t/\tau_\Delta)), \quad (1)$$

and τ_T is the lifetime of the triplet states obtained from transient absorption measurements.

Fig. 6 Transient absorption spectra of ZnPc in **1** ($\lambda_{exc}=658$ nm) (**a**) and ZnTPP in **2** ($\lambda_{exc}=425$ nm) (**b**) at 10 μs after excitation in air atmosphere

Table 1 Average fluorescence lifetimes (τ_F) of ZnTPP, lifetimes of the triplet states (τ_T) in argon atmosphere, rate constants for quenching of the triplet states by oxygen (k_q), and lifetime of $O_2(^1\Delta_g)$ (τ_Δ) in nanofabrics **1–4**

Nanofabric		Singlet states	Triplet states		O_2 $(^1\Delta_g)$
No.	Photosensitizer	τ_F (ns)	τ_T (μs)[a]	k_q (s^{-1}Pa^{-1})	τ_Δ (μs) [b]
1	ZnPc	–	540±50	1.4±0.1	12.9±3
2	ZnTPP	5.29	430±30	1.3±0.1	15.4±3
3	Mixture of ZnPc, ZnTPP	1.79	480±50	1.3±0.1	15.2±3
4	ZnPc, ZnTPP in two layers	3.07	530±60	1.4±0.1	17.0±4

[a] ZnTPP was excited at 425 or 308 nm with the detection of the triplet states at 460 nm, ZnPc was excited at 658 and 308 nm and the triplet states were detected at 500 nm
[b] Calculated using Eq. (1) in air and oxygen atmosphere, τ_T was fixed to the values obtained from transient absorption measurements

An example of the singlet oxygen luminescence signal is depicted in Fig. 7. The results of the fitting procedures (Table 1) indicate the similar lifetimes of O_2 $(^1\Delta_g)$ in all nanofabrics **1–4**. The values of τ_Δ are slightly lower than those of TPP in the PUR matrix (τ_Δ=21.2 μs) [10].

Photooxidation of inorganic and organic compounds

The photophysical measurements described above proved the ability of porphyrin or phthalocyanine sensitizers in nanofibers to form the triplet states and $O_2(^1\Delta_g)$. Singlet oxygen $O_2(^1\Delta_g)$ is a short-lived species especially in polar media having a lifetime $\tau_\Delta\sim3.5$ μs in water [11]. The mean radial diffusion length of $O_2(^1\Delta_g)$, l_r, can be estimated using the equation $l_r = (6D_0\tau_\Delta)^{1/2}$, where D_0 is the diffusion coefficient for oxygen in water (2.07×10^{-5} cm^2 s^{-1}) [25, 26]. The low value of about 210 nm in water over the period of the singlet oxygen lifetime indicates that the adsorption on the surface or the close contact of target molecules with nanofibers is a fundamental prerequisite for the effective course of photooxidation reactions. Hence, electrostatic and hydrophobic forces between photosensitizer and the PUR matrix can play an important role in photooxidation and photodynamic processes.

The photooxidation ability of doped nanofibers was tested by the sensitive method based on the photooxidation of I^- to I_3^-. The photoproduced concentration of I_3^- is proportional to the concentration of $O_2(^1\Delta_g)$ [27]. The relative photooxidation efficacy (PE) of nanofabrics **1–4** was calculated as $A(I_3^-)/\sum I_0(1-10^{-Ai})$, where $A(I_3^-)$ is the absorbance of photoproduced I_3^- at 351 nm after 10 min of irradiation and $\sum I_0(1-10^{-Ai})$ is the sum of absorbed light intensities at all wavelengths λ_i, and was compared with the nanofabric doped by TPP (Table 2) [10].

The PE values increase in D_2O because the effective lifetime of $O_2(^1\Delta_g)$ increases about ten times when compared to that in H_2O. In addition, the efficacy is nearly zero in the presence of NaN$_3$ (>0.01 mol l^{-1}), an effective quencher of $O_2(^1\Delta_g)$. As follows from Table 2, the PE values are proportional to the intensity of incident light

indicating that the photoxidation is not directed by the actual concentration of oxygen in the polymer matrix, but it is governed by the intensity of absorbed light. No photooxidation was observed in the dark, upon irradiation in the absence of dissolved oxygen, or upon irradiation of the photosensitizer-free nanofabrics. All these results confirm the importance of the photoactive molecules imbedded in the PUR matrix. Nanofabric containing TPP appears to be more effective photosensitizing material compared with **1** or **2**, although all used sensitizers have similar quantum yields of the $O_2(^1\Delta_g)$ formation in solutions [11]. Nanofabrics **3** and **4** exhibit a mean photooxidation efficacy (Table 2). Similar PE values were obtained for the photooxidation of sodium salt of uric acid (not shown).

The photostability of imbedded sensitizers is an important factor for nanofabrics applications. Therefore, the kinetics of ZnPc and ZnTPP photodegradation was evaluated using decreasing absorption bands of the photosensitizers during the irradiation in air or N_2 atmosphere. The corresponding rate constants of photodegradation were
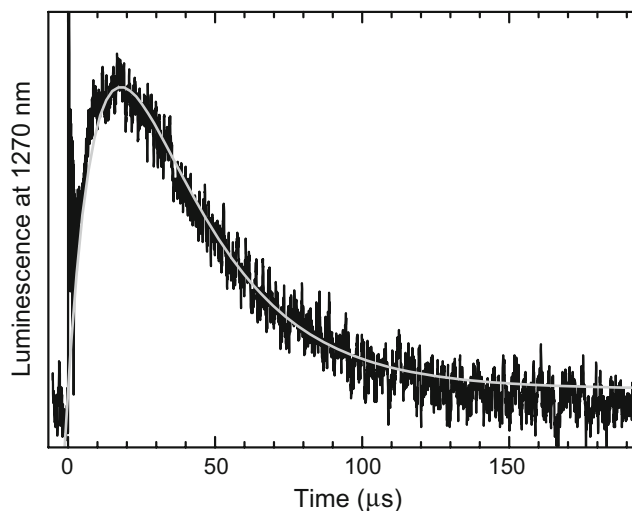
Fig. 7 Phosphorescence of $O_2(^1\Delta_g)$ and the least-square fit of Eq. (1) to the experimental data (grey line): ZnPc in nanofabric **1** was excited at 658 nm and emitted phosphorescence was collected at 1,270 nm as a difference between the measurement in air and in argon atmosphere

Table 2 Relative light intensity (I_{rel}), relative photooxidation efficacy (PE) of I^- to I_3^- photooxidation in aqueous solutions, and photostability of nanofabrics **1–4** in air atmosphere expressed by the rate constant of photodegradation (k_P)

No.	Nanofabric Photosensitizer	I_{rel} (a.u.)	PE^a (a.u.)	k_P^a (min^{-1})
1	ZnPc	1	0.58	0.013
1	ZnPc	1	0.79[b]	–
1	ZnPc	1	0.06[c]	–
1	ZnPc	0.5	0.3	–
1	ZnPc	0.2	0.12	–
1	ZnPc	0.02	0.01	–
2	ZnTPP	1	0.33	0.028
3	ZnPc,ZnTPP in one layer	1	0.49	0.027 (ZnTPP) 0.012 (ZnPc)
4	ZnPc,ZnTPP in two layers	1	0.41	0.027 (ZnTPP) 0.012 (ZnPc)
	TPP	1	1	0.0008

[a] Estimated error 20%
[b] In 50% D$_2$O
[c] NaN$_3$ (0.01 mol l^{-1})

calculated using the monoexponential equation $A_t = A_0 \times \exp(-k_P\,t)$, where A_t and A_0 are the absorbance of the photosensitizer at time t and before irradiation, respectively. Both ZnPc and ZnTPP photodecompose faster in air atmosphere than TPP (Table 2). The observation correlates with the fact that zinc porphyrinoids are sensitive to photooxidation by $O_2(^1\Delta_g)$ [28]. While ZnPc in **1**, **3** and **4** appears to be photostable in oxygen-free atmosphere, ZnTPP encapsulated in **2–4** photodegrades (Fig. 8) documenting the presence of a further photodegradation channel based probably on electron transfer between excited ZnTPP and PUR polymer. It is likely that electron transfer to polymer competes with the $O_2(^1\Delta_g)$ formation in
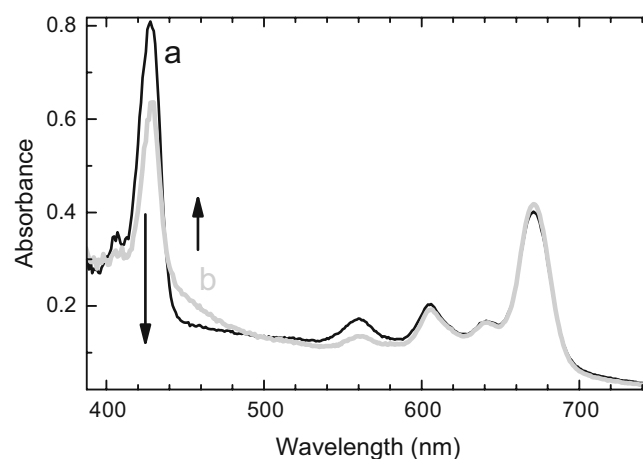
Fig. 8 UV/Vis spectra of **3** in nitrogen atmosphere before (**a**) and after 60 min of irradiation by a stabilized 300 W halogen lamp (**b**, *grey line*). The arrows show changes in the UV/Vis spectrum that document the photodegradation of ZnTPP

1, 3, and **4** and cause a lower photooxidation efficacy and photostability when compared with the TPP-based nanofabric (Table 2).

The stability of the pthtalocyanine/porphyrin photosensitizers might be increased by a useful structural modification e.g. the replacement of the C–H bonds with C–F bonds increases the robustness of the overall ring but immune to attack by singlet oxygen [29].

Photodynamic effects to bacteria on nanofabric surfaces

To evaluate the bactericidal effects of $O_2(^1\Delta_g)$ at the surface of nanofabrics **1–4** the modified method developed recently was used [10]. Two pieces of nanofabrics were placed on bacterial agar plates: photosenzitizer-doped nanofabric and control nanofabric without photosensitizer. Both pieces were inoculated with drops containing bacteria *Escherichia coli* in a suspension. Two identical agar plates with nanofabrics and bacteria were prepared for each experiment (Fig. 9). One plate was illuminated with cold white light for 30 min (plate A), while the second (plate B) was kept in the dark. After overnight incubation, bacteria grew only on the control nanofabric on the illuminated plate A. In contrast on the plate B kept in the dark, bacterial colonies grew in the inoculated spots on both nanofabrics. Each experiment was repeated at least six times. Similar results were obtained with nanofabrics **1**, **2** and **4** (data not shown). We conclude that photosensitizer-doped nanofabrics produce enough $O_2(^1\Delta_g)$ to kill bacteria on their surfaces when exposed to white light.

Conclusions

The PUR nanofabrics containing ZnPc and ZnTPP are efficient light-harvesting systems, in which both chromophores absorb a wide range of visible light with large
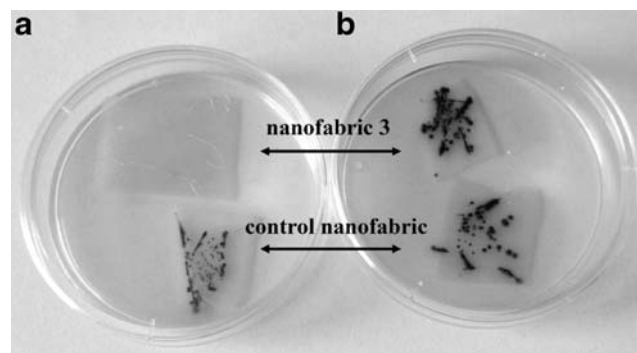
Fig. 9 Photodynamic effect of the nanofabric **3** on bacteria *E. coli*: Agar plates with pieces of **3** and a control nanofabric without photosensitizer inoculated with *E. coli* exposed to light (**a**), and kept in the dark (**b**)

extinction coefficients. Both ZnPc and ZnTPP are stabilized by the ligation of Zn atoms with the imide or carbonyl groups of the PUR polymer and stay monomeric in the PUR matrices. The photoexcitation of nanofabrics leads to efficient energy transfer from the ZnTPP singlet states to ZnPc followed by intersystem crossing to the triplet states and by the generation of singlet oxygen. The PUR nanofabrics doped by ZnPc and ZnTPP readily photooxidize inorganic and organic substrates and have bactericidal effects on their surfaces, however, these nanofabrics are less efficient and photostable than nanofabrics doped by free-base porphyrin TPP.

References

1. Maisch T, Baier J, Franz B, Maier M, Landthaler M, Szeimies RM, Bäumler W (2007) The role of singlet oxygen and oxygen concentration in photodynamic inactivation of bacteria. Proc Natl Acad Sci USA 104:7223–7228 doi:10.1073/pnas.0611328104
2. Patrice T (2004) Photodynamic therapy. Royal Society of Chemistry, London
3. Lissi MV, Encias E, Lemp E, Rubio MA (1993) Singlet oxygen $O_2(^1\Delta_g)$ bimolecular processes-solvent and compartmentalization effect. Chem Rev 93:699–723 doi:10.1021/cr00018a004
4. Lang K, Mosinger J, Wagnerová DM (2004) Photophysical properties of porhyrinoid sensitizers non-covalently bound to host molecules; models for photodynamic therapy. Coord Chem Rev 248:321–350 doi:10.1016/j.ccr.2004.02.004
5. Schweitzer C, Schmidt R (2003) Physical mechanisms of generation and deactivation of singlet oxygen. Chem Rev 103:1685–1758 doi:10.1021/cr010371d
6. Wilkinson F, Helman WP, Ross AB (1995) Rate constants for the decay and reactions of the lowest electronically excited singlet state of molecular oxygen in solution. An expanded and revised compilation. J Phys Chem Ref Data 24:663–1021
7. Voeikov VL (2005) Biological oxidation: over a century of hardship for the concept of active oxygen. Cell Mol Biol 51:663–675
8. McGlinchey SM, McCoy CP, Gorman SP, Jones DS (2008) Key biological issues in contact lens development. Expert Rev Med Devices 5:581–590 doi:10.1586/17434440.5.5.581
9. Brady C, Bell SEJ, Parsons C, Gorman SP, Jones DS, McCoy CP (2007) Novel porphyrin-incorporated hydrogels for photoactive intraocular lens biomaterials. J Phys Chem B 111:527–534 doi:10.1021/jp066217i
10. Mosinger J, Jirsák O, Kubát P, Lang K, Mosinger B Jr (2007) Bactericidal nanofabrics based on photosensitized formation of singlet oxygen. J Mater Chem 17:164–166 doi:10.1039/b614617a
11. Wilkinson F, Helman WP, Ross AB (1993) Quantum yields for the photosensitized formation of the lowest electronically excited singlet state of molecular oxygen in solution. J Phys Chem Ref Data 22:113–262
12. Arnbjerg J, Johnsen M, Nielsen CB, Jorgensen M, Ogilby PR (2007) Effect of sensitizer protonation on singlet oxygen production in aqueous and nonaqueous media. J Phys Chem A 111:4573–4583 doi:10.1021/jp066843f
13. Ricchelli F (1995) Photophysical properties of porphyrins in biological membranes. J Photochem Photobiol B Biol 29:109–118 doi:10.1016/1011-1344(95)07155-U
14. Jirsák O, Sanetrník F, Lukáš D, Kotek V, Martinová L, Chaloupek J, CZ pat. 294274 (2003);PCT/CZ2004/000056 (2004)
15. Kapusta P, Wahl M, Benda A, Hof M, Enderlein J (2007) Fluorescence lifetime correlation spectroscopy. J Fluoresc 17:43–48 doi:10.1007/s10895-006-0145-1
16. Lukaszewicz A, Karolczak J, Kowalska D, Maciejewski A, Ziolek M, Steer RP (2007) Photophysical processes in electronic states of zinc tetraphenyl porphyrin accessed on one- and two-photon excitation in the soret region. Chem Phys 331:359–372 doi:10.1016/j.chemphys.2006.11.006
17. Rogers JE, Nguyen KA, Hufnagle DC, McLean DG, Su W, Gossett KM, Burke AR, Vinogradov SA, Pachter R, Fleitz PA (2003) Observation and interpretation of annulated porphyrins: studies on the photophysical properties of meso-tetraphenylmetalloporphyrins. J Phys Chem A 107:11331–11339 doi:10.1021/jp0354705
18. Rajesh CS, Capitosti GJ, Cramer SJ, David A, Modarelli DA (2001) Photoinduced electron-transfer within free base and zinc porphyrin containing poly(amide). Dendrimers J Phys Chem B 105:10175–10188 doi:10.1021/jp010575y
19. Ogunsipe A, Maree D, Nyokong T (2003) Solvent effects on the photochemical and fluorescence properties of zinc phthalocyanine derivatives. J Mol Struct 650:131–140 doi:10.1016/S0022-2860(03)00155-8
20. Ito F, Ishibashi Y, Khan SR, Miyasaka H, Kameyama K, Morisue M, Satake A, Ogawa K, Kobuke Y (1996) Photoinduced electron transfer and excitation energy transfer in directly linked zinc porphyrin/zinc phthalocyanine composite. Langmuir 12:2932–2938 doi:10.1021/la960240l
21. Kroon JM, Koehorst RBM, vanDijk M, Sanders GM, Sudhölter EJR (1997) Self-assembling properties of non-ionic tetraphenylporphyrins and discotic phthalocyanines carrying oligo(ethylene oxide) alkyl or alkoxy units. J Mater Chem 7:615–624 doi:10.1039/a605328i
22. Lakowicz JR (1983) Principles of fluorescence spectroscopy. Plenum, New York
23. Carmichael I, Hug GL (1986) Triplet–triplet absorption spectra of organic molecules in condensed phases. J Phys Chem Ref Data 15:1–250
24. Ricciardi G, Rosa A, Baerends EJ (2001) Ground and excited states of zinc phthalocyanine studied by density functional methods. J Phys Chem A 105:5242–5254 doi:10.1021/jp0042361
25. Ijeri VS, Daasbjerg K, Ogilby PR, Poulsen L (2008) Spatial and Temporal Electrochemical Control of Singlet Oxygen Production and Decay in Photosensitized Experiments. Langmuir 24:1070–1079 doi:10.1021/la7028577
26. Tsushima M, Tokuda K, Ohsaka T (1994) Use of hydrodynamic chronocoulometry for simultaneous determination of diffusion coefficients and concentrations of dioxygen in various media. Anal Chem 66:4551–4556 doi:10.1021/ac00096a024
27. Mosinger J, Mosinger B (1995) Photodynamic sensitizers assay: rapid and sensitive iodometric measurement. Experientia 51:106–109 doi:10.1007/BF01929349
28. Hof FR, Whitten DG (1975) In: Smith KM (ed) Porphyrins and Metalloporphyrins. Elsevier, Amsterdam, pp 667–695
29. Keizer SP, Bench BA, Gorun SM, Stillman MJ (2003) Spectroscopy and Electronic Structure of Electron Deficient Zinc Phthalocyanines. J Am Chem Soc 125:7067–7085 doi:10.1021/ja0299710